5 Modeling and Analysis of Short Waves[1]

Wind waves and swell that are generated by local or distant storms are defined as short waves. These surface gravity waves have periods less than about 25 sec. Quantitative information about short waves at the Willapa Bay entrance is required in this study for determining navigability and estimating sediment transport for evaluating navigation channel alternatives. Wave height, period, and direction (relative to the channel orientation) in part determine navigability. Sediment transport, which determines the frequency and cost of channel maintenance, is driven by a combination of short waves and currents as discussed in Chapter 6.

The purpose of this chapter is to describe modeling of the transformation of short waves across the Willapa bar and into the bay. First, the wave climate offshore of Willapa Bay is described. The offshore climate provides boundary conditions to initialize the wave model. Next, the STeady-state spectral WAVE transformation model STWAVE is described. STWAVE is based on the conservation of wave action, and it includes depth- and current-induced refraction, shoaling, and wave breaking. The bathymetry grid used in the model is presented next. Accurate bathymetry information is required, as discussed in Chapter 2, because waves refract and shoal according to the configuration of the sea bottom. The wave model is then evaluated with field measurements obtained in Chapter 4. Finally, simulations of the nearshore waves for evaluating channel design alternatives are presented.

Wave Climate

The first step in evaluating alternatives for the Willapa navigation channel is to define the wave climate seaward of the inlet, in relatively deep water. The offshore wave climate provides representative wave boundary conditions that initiate the wave transformation model. The model can then estimate the variation in wave height and direction along the channel. For highest accuracy, the source of wave information used to develop the offshore wave climate should be a site near Willapa Bay. Also, the water depth should be sufficient to avoid depth-limited breaking and refraction and shoaling induced by local nearshore contours or shoals. The source of wave data must have a long record (for

[1] Written by Dr. Jane McKee Smith and Mr. Bruce A. Ebersole, U.S. Army Engineer Research and Development Center, Coastal and Hydraulics Laboratory, Vicksburg, MS.

accurate climate statistics) and be presently operating (to facilitate verification with 1998 data collected at Willapa).

Offshore wave information near Willapa Bay is available from four sources:

a. Directional wave buoy offshore of Grays Harbor, Washington. This is a Datawell buoy located at 46°51.4'N, 124°14.7'W, in a depth of 40.2 m (Station 03601). The buoy is supported by U.S. Army Engineer District, Seattle, through the Corps of Engineers Field Wave Gauging Program and operated by the Scripps Institute of Oceanography (SIO), Coastal Data Information Program (CDIP). The buoy was installed in 1993 and is still operating.

b. Bottom-mounted slope array offshore of Long Beach, Washington. The slope array was located at 46°23.2'N, 124°4.7'W, in a depth of 10 m (Station 05401). The gauge was supported by the Corps of Engineers Field Wave Gauging Program and operated by the SIO CDIP. The gauge was installed in 1983 and operated until mid-1995.

c. Directional wave buoy offshore of the Columbia River Bar, Oregon. This is a 3-m discus buoy located at 46 7'N, 124°30'W, in a depth of 128 m (Station 46029). The buoy is supported and operated by the National Data Buoy Center. The buoy was installed in 1984 and is still operating.

d. The U.S. Army Corps of Engineers' Wave Information Study (WIS) wave hindcast. The closest WIS Phase II station is located at 46°16.2'N, 124°46.2'W, in deep water (Station 46) (Corson et al. 1987). The WIS hindcast covers the period 1956-1975.

The Grays Harbor buoy and the Long Beach gauge are located closest to Willapa Bay. The Grays Harbor buoy is approximately 20 km northwest of the Willapa entrance, and the Long Beach gauge was about 30 km south of the entrance. Because the Long Beach gauge was in relatively shallow water, wave direction was strongly influenced by the local bathymetry, and the higher waves would break at the site, biasing the distribution of the highest wave heights. Also, the Long Beach gauge is no longer operational, so evaluation of the wave model with wave data collected at the inlet in 1998 cannot use the Long Beach gauge for incident wave conditions. The Columbia River Bar buoy and the WIS information provide longer periods of records than the Grays Harbor buoy, but are also much further away from Willapa Bay. Also, the WIS information does not overlap with the 1998 Willapa Bay measurements for evaluation of the model. For these reasons, the Grays Harbor buoy was selected to determine the wave climate for Willapa Bay. Appendix E contains comparisons of wave climate statistics from the Grays Harbor buoy, the Long Beach slope array, and the Columbia River buoy.

A wave climate was developed using Grays Harbor data from September 1996 through August 1998. In September 1996, the reporting of wave angles changed from an arithmetic weighted average to a peak wave direction (wave direction band with the maximum energy). Thus, for consistency, only the newer data were used. Although a 2-year data record is short for describing extreme wave statistics, it is sufficient to characterize waves for navigation and typical storms to assess channel shoaling. To construct the wave climate, percent

occurrence tables (broken down by height, period, and direction) were calculated for each month of data and then the monthly tables were combined, giving equal weight to each month. The equal monthly weighting takes into account gaps in the data and changes in sampling frequency. The Grays Harbor wave climate is illustrated in Figure 5-1 as a wave rose with directional resolution of 22.5 deg. Table 5-1 shows overall distributions by height, period, and direction.

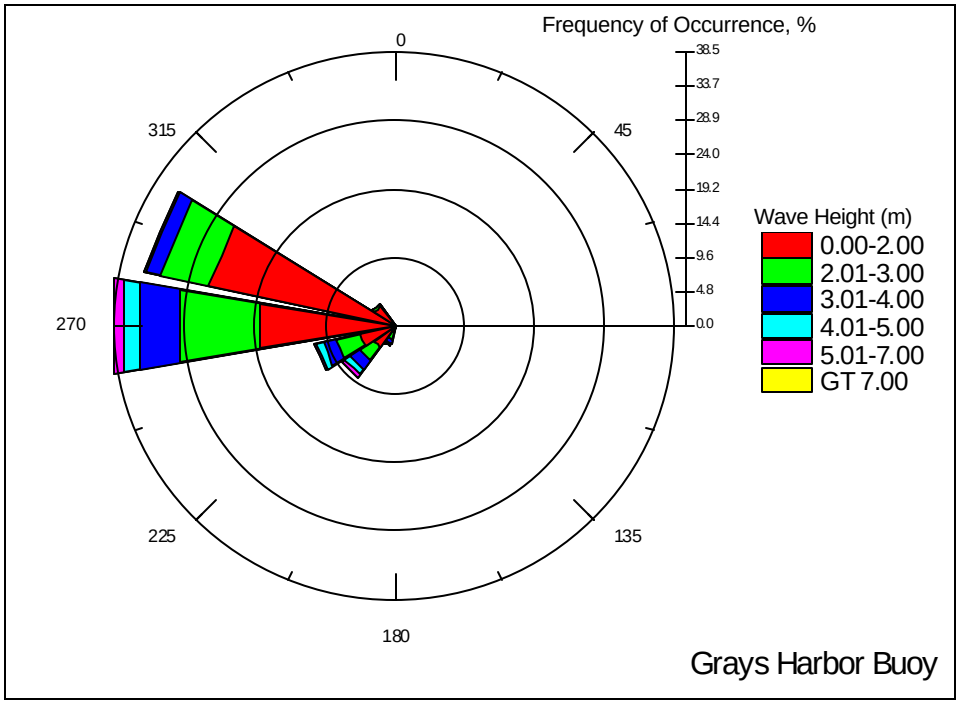

Figure 5-1. Grays Harbor buoy wave rose

Table 5-1
Grays Harbor Wave Distribution by Height, Period, and Direction

Height m	Occurrence percent	Period sec	Occurrence percent	Direction deg	Occurrence percent
0.00-2.0	57.5	0.00- 6.0	2.8	180.0	0.4
2.01-3.0	24.7	6.01-10.0	52.2	202.5	2.7
3.01-4.0	11.1	10.01-14.0	28.1	225.0	8.7
4.01-5.0	4.4	14.01-18.0	13.8	247.5	11.2
5.01-7.0	2.2	>18.01	3.1	270.0	38.5
>7.01	0.1			292.5	34.6
				315.0	3.7
				337.5	0.1

The average conditions over the period August 1993 through July 1999 were wave height of 6.9 ft, peak period of 10.6 sec, and peak direction of 273 deg (based on wave data revised by CDIP in the spring of 1999). A monthly distribution of the mean and maximum wave heights, periods, and directions and occurrence of heights less than 9 ft are given in Table 5-2 (maximum period and direction given in the table are the values associated with the maximum wave height). The maximum wave height in the record is 29.6 ft, with a period of 13.3 sec and direction of 234 deg (24 November 1998 at 0719 Greenwich mean time (GMT)). Large winter storms impede navigation at the Willapa entrance channel. Based on the Grays Harbor buoy, wave height exceeds 9.8 ft 42 percent of the time and exceeds 4.9 ft 92 percent of the time during winter months (December-February). Time-histories of winter wave heights and directions from the Grays Harbor buoy are given in Appendix C.

Table 5-2
Mean and Maximum Wave Parameters Measured at Grays Harbor Buoy (August 1993 - July 1999)

Month	Mean Height ft	Mean Period sec	Mean Direction deg	Occurrence of H ≤ 9 ft percent	Maximum Height ft	Maximum Period[1] sec	Maximum Direction[1] deg
January	8.83	11.6	257	57	27.8	13.3	258
February	9.84	13.0	261	48	24.3	13.3	269
March	8.14	12.0	264	63	23.1	12.5	238
April	6.92	11.0	274	79	18.2	11.1	290
May	5.54	9.4	278	95	13.3	11.8	278
June	5.15	9.4	283	95	11.6	15.4	261
July	4.27	8.1	287	99	11.3	10.0	300
August	3.84	8.5	283	100	9.8	9.1	283
September	5.28	9.6	282	95	12.2	11.8	281
October	6.92	10.9	275	78	21.3	12.5	269
November	9.12	11.1	264	58	29.6	13.3	234
December	10.50	12.4	264	36	25.7	14.3	272

[1]Value associated with the maximum wave height.

Wave Transformation Model

The numerical model STWAVE (Resio 1987, 1988; Smith, Resio, and Zundel 1999) was used to transform waves across the Willapa bar for evaluation of channel alternatives. STWAVE numerically solves the steady-state conservation of spectral action balance along backward-traced wave rays:

$$(C_{ga})_x \frac{\partial}{\partial x} \frac{C_a C_{ga} \cos(m-a) E(f,a)}{w_r} + (C_{ga})_y \frac{\partial}{\partial y} \frac{C_a C_{ga} \cos(m-a) E(f,a)}{w_r} = \sum \frac{S}{w_r} \quad (5\text{-}1)$$

where

C_{ga} = absolute wave group celerity

x,y = spatial coordinates; subscripts indicate x-and y-components

C_a = absolute wave celerity

m = current direction

α = propagation direction of spectral component

E = spectral energy density

F = frequency of spectral component

T_r = relative angular frequency (frequency relative to the current)

S = energy source/sink terms

The source terms include wind input, nonlinear wave-wave interactions, dissipation within the wave field, and surf-zone breaking. The terms on the left-hand side of Equation 5-1 represent wave propagation (refraction and shoaling), and the source terms on the right-hand side of the equation represent energy growth or decay in the spectrum.

The assumptions made in STWAVE are as follows:

a. Mild bottom slope and negligible wave reflection.

b. Spatially homogeneous offshore wave conditions.

c. Steady waves, currents, and winds.

d. Linear refraction and shoaling.

e. Depth-uniform current.

f. Negligible bottom friction.

STWAVE is a half-plane model, meaning that only waves propagating toward the coast are represented. Waves reflected from the coast or waves generated by winds blowing offshore are neglected. Wave breaking in the surf zone limits the maximum wave height based on the local water depth and wave steepness:

$$H_{mo_{\max}} = 0.1L \tanh kd \tag{5-2}$$

where

H_{mo} = zero-moment wave height

L = wavelength

k = wave number

d = water depth

STWAVE is a finite-difference model and calculates wave spectra on a rectangular grid with square grid cells. The model outputs zero-moment wave

height, peak wave period T_p, and mean wave direction α_m at all grid points and two-dimensional spectra at selected grid points.

Wave Model Inputs

The inputs required to execute STWAVE are as follows:

a. Bathymetry grid (including shoreline position and grid size and resolution).

b. Incident frequency-direction wave spectrum on the offshore grid boundary.

c. Current field (optional).

d. Tide elevation, wind speed, and wind direction (optional).

Bathymetry grid

Both the wave and circulation models (Chapter 6) require bathymetry data to construct computational grids over which the waves propagate and transform. Accurate bathymetry is required for modeling waves at Willapa Bay because the complex shoals control transformation and breaking. Bathymetry data collected in this study include high-resolution Lidar surveys with Scanning Hydrographic Operational Airborne Lidar Survey (SHOALS) (Lillycrop, Parson, and Irish 1996) and broad-coverage surveys collected by the Seattle District survey boat, the *Shoalhunter*. These data were combined with existing National Ocean Service (NOS) data to provide coverage of the nearshore, bar, and bay (Chapter 3).

Very shallow areas across the Willapa bar could not be surveyed because of continuous wave breaking. Bathymetry in these areas was estimated from local knowledge.[1,2] A bathymetry grid for the circulation model was generated from the combined SHOALS, *Shoalhunter*, and NOS data to represent the existing conditions at Willapa (see Chapter 6). For wave modeling, the unstructured circulation model grid was linearly interpolated onto a rectilinear STWAVE grid. The STWAVE grid has a resolution of 100 m, with 301 grid cells across the shore and 511 cells along the shore. The area of coverage is 30 km (west to east) by 51 km (south to north). The grid origin (southwest corner of the grid) is located at the Universal Transverse Mercator (UTM) Northing 5,136,069 m (lat. 46.3719°N) and Easting 407,546 m (long. 124.2021°W). The existing condition bathymetry and STWAVE grid coverage are shown in Figure 5-2. Depths are given in meters relative to the mean tide level (mtl). Note that other chapters typically reference depths to mean lower low water (mllw) datum, and a value of 1.52 m mllw was used to convert depths to mtl based on the tidal datum at Toke Point. In addition to the grid generated for existing bathymetry, grids were developed in the same manner for Alternatives 3A, 3B, 4A, and 3H. Each of these grids incorporates modifications to the existing bathymetry that correspond to the particular alternative.

[1] Personal Communication, October 1998, Mr. Thomas Landreth, *Shoalhunter* Captain, U.S. Army Engineer District Seattle, Seattle, WA.
[2] Personal Communication, October 1998, Mr. Randy D. Lewis, City Administrator, Westport, WA.

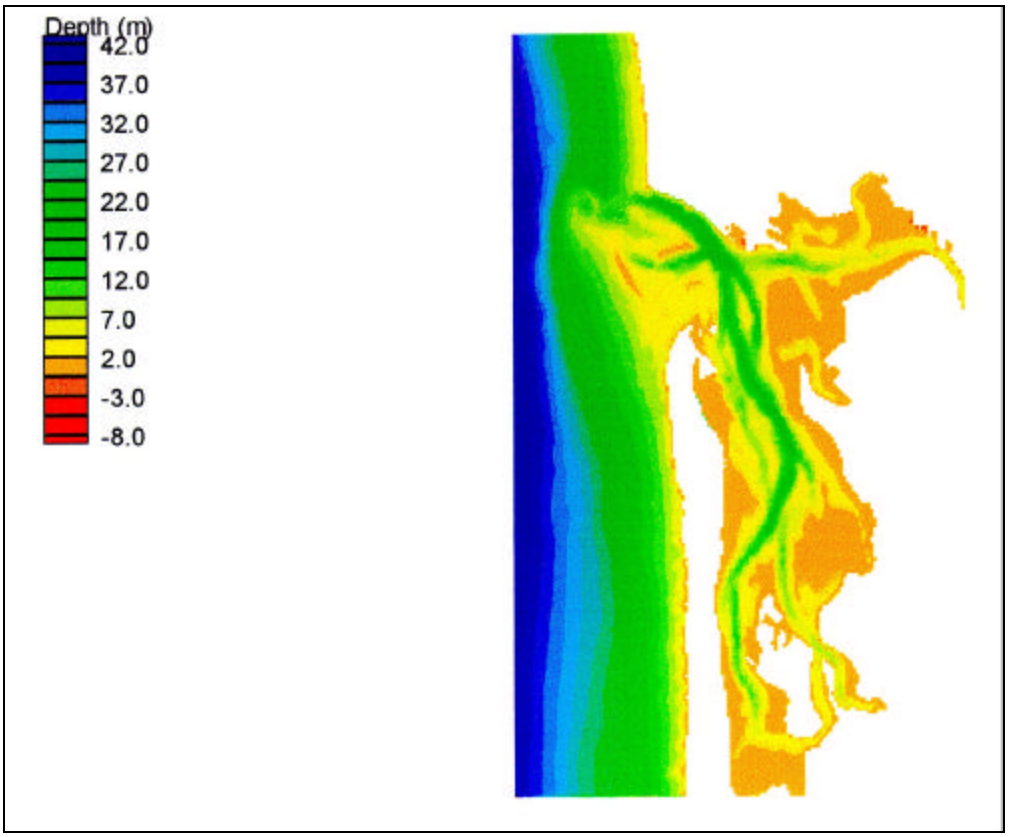

Figure 5-2. STWAVE existing condition bathymetry grid

Input wave spectra

Input wave spectra are the forcing for the wave model and provide the distribution of wave energy as a function of frequency and direction. For this project, the input spectra were generated in two ways:

a. Verification spectra. For evaluation of the wave model with field measurements (1-4 September 1998, 15-20 October 1998, and 11-16 November 1998), one-dimensional frequency spectra from the Grays Harbor buoy were used. The directional distributions measured at the buoy lack sufficient resolution to drive the model, so a theoretical distribution of the form $\cos^{nn}(a - a_m)$ was applied, where *nn* is the spreading coefficient, and a_m is the mean wave direction. The values used for *nn* are given in Table 5-3 (Thompson et al. 1996). Large values of *nn* indicate a narrow directional distribution (swell waves), and small values represent a wide distribution (sea waves). The value of *nn* for the peak of the spectrum (Table 5-3) was applied for the peak and lower frequencies. For frequencies higher than the peak, the values in Table 5-3 were applied.

Table 5-3
Values of *nn* Defining Direction Distribution in Verification Spectra

f, Hz	≤ 0.04	0.045	0.05	0.055	0.06	0.08	≥ 0.1
nn	38	36	30	26	22	10	4

b. Representative spectra. For model runs made to evaluate channel alternatives and sediment-transport potential, representative wave spectra were generated. These spectra are representative of the height, period, and direction ranges shown in Table 5-1. The spectra were generated with a TMA[1] frequency distribution (Bouws et al. 1985) and a $\cos^{nn}(\alpha - \alpha_m)$ directional distribution. The TMA shape is defined by the wave height, peak period, and spectral peakedness parameter *g*. Large values of *g* indicate a narrow frequency distribution (swell waves), and small values represent a wide distribution (sea waves). Combinations of *g* and *nn* used to generate the representative spectra are given as a function of peak period in Table 5-4.

Table 5-4
Values of (and *nn* Defining Representative Spectra

T_p (sec)	5	8	12	16	20
g	3.3	3.3	4	6	8
nn	4	4	10	20	30

Current fields

For applications where wave-current interaction significantly alters the wave height or blocks the waves, current fields are needed as an input to the model. Wave height increases on strong ebb currents and decreases on strong flood currents. Currents also alter wave direction. The current modifies waves with higher frequencies (shorter periods) more than it does waves with lower frequencies. In addition to shoaling and refraction by currents, wave breaking is also changed by an opposing or following current (*L* and *k* change in Equation 5-2). Wave breaking is enhanced on an opposing current (ebb) and reduced on a following current (flood). If the ebb current is strong, waves with short periods cannot propagate against it, and wave energy is blocked and dissipated.

For Willapa, model runs with and without a current were made to assess the sensitivity of the wave transformation at the study site to wave-current interaction. For the sensitivity analysis, relatively commonly occurring short- and long-period waves at Willapa Bay were selected: H_{mo} = 1.5 m, T_p = 8 sec, and α_m = 292.5 deg (probability of occurrence of 21.6 percent) and H_{mo} = 2.5 m,

[1] Named for the three data sets used to develop the spectrum: TEXEL storm, MARSEN, and ARSLOE.

T_p = 16 sec, and a_m = 270 deg (probability of occurrence of 2.9 percent). The waves were run for a typical peak ebb and flood, and the first wave was also run for a maximum spring tide ebb and flood.

Figures 5-3 and 5-4 are plots of the difference in wave height with and without current for the first wave and typical ebb and flood conditions, respectively (Cases 1 and 2 in Table 5-5). The increase in wave height on the outer bar for a typical ebb is about 2 ft (0.6 m), which is equal to the value estimated based on local knowledge.[1] Table 5-5 summarizes the maximum differences in wave height (height modified by the current minus height neglecting current) for ebb and flood currents. The percent differences are calculated as the difference in wave height calculated with and without currents divided by the height calculated without currents.

Table 5-5
Sensitivity Analysis of Wave Transformation to Current

Case	Incident Wave Conditions			Max North Channel Current	Max Wave Height Difference	Max Wave Height Difference
	H_{mo} m	T_p sec	a_m deg	m/sec	m	percent
1	1.5	8	292.5	1.6 ebb	0.6	67
2	1.5	8	292.5	1.4 flood	-0.2	-15
3	2.5	16	270	1.6 ebb	0.4	17
4	2.5	16	270	1.4 flood	-0.4	-9
5	1.5	8	292.5	2.0 ebb	0.8	79
6	1.5	8	292.5	1.6 flood	-0.2	-16

[1] Personal Communication, October 1998, Mr. Randy D. Lewis, City Administrator, Westport, Washington. Mr. Lewis has served in the U.S. Coast Guard and is familiar with the channels and sea state at the Willapa entrance.

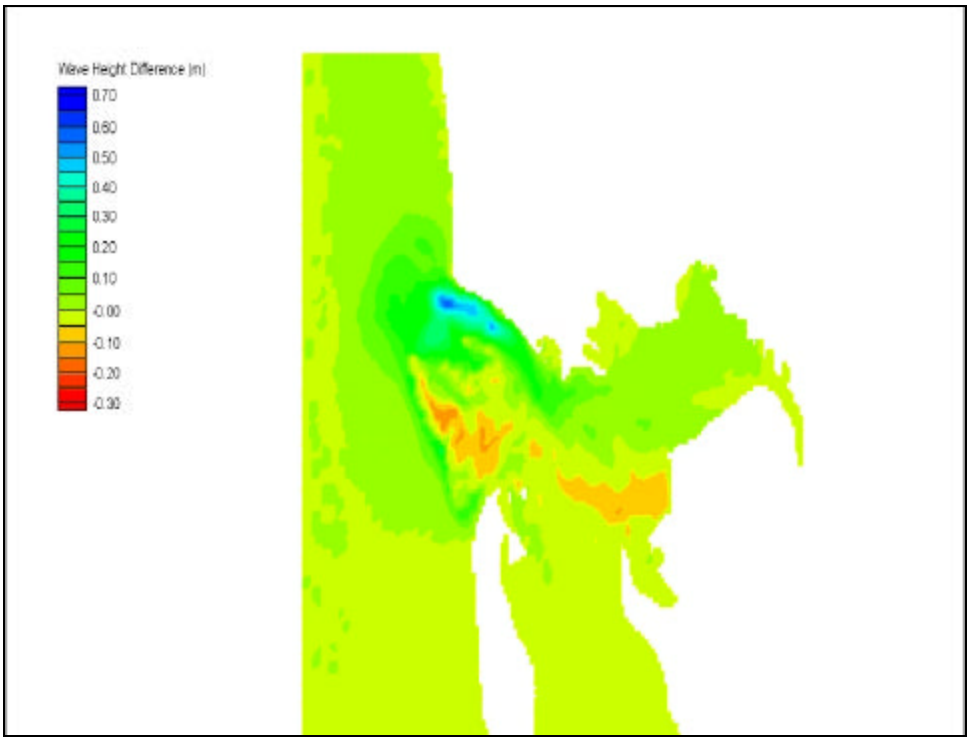

Figure 5-3. Wave height with ebb current minus wave height with no current

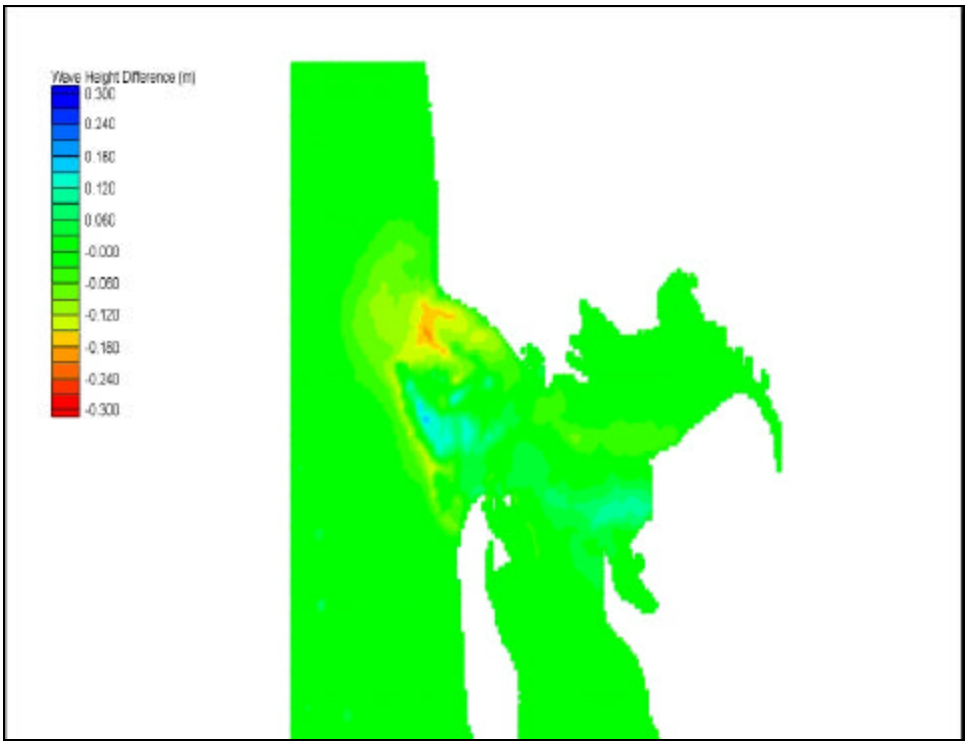

Figure 5-4. Wave height with flood current minus wave height with no current

The maximum differences in wave height with and without current are significant (0.4 to 0.8 m on ebb and 0.2 to 0.4 m on flood). The largest differences occur in the North Channel through the bar, so by the present sensitivity analysis, wave-current interaction should be included in evaluation of navigability. However, the model shows that the regions where wave-current interaction is significant are fairly small. Regions of wave-height differences greater than 30 percent (peak ebb) were seven grid cells wide (700 m) or less (which is less than 9 percent of the inlet width). Thus, wave-current interaction need not be considered in estimating channel shoaling, which is determined more by wave breaking, wave-driven currents, and sediment transport on the ebb shoals than by wave height in the navigation channel. Wave-current interaction was included for wave model runs to assess navigability, but this intensive, iterative calculation was neglected for runs performed to provide sediment transport forcing.

Tide and wind

Tide elevation is applied in STWAVE as constant water depth change over the entire grid. Within the Willapa grid domain, the tide elevation does vary spatially, but the influence of this variation on wave transformation is relatively small (and is on the order of wind and wave setup, which are neglected). Tide elevation for wave runs is specified from either tide measurements at the NOS Toke Point station or, for typical conditions, set to mtl (0 m), mean low water (mlw) (-1 m), or mean high water (mhw) (+1 m). Because the grid depths are specified relative to mtl, tide fluctuations are specified relative to mtl.

Wind input in STWAVE creates wave growth across the grid domain. Wave measurements at the Grays Harbor buoy contain most of the local wave-generation processes. Fetch lengths from the buoy depth (40 m) to the Willapa entrance are short, so additional growth would be small. Thus, local generation is neglected in the STWAVE calculations, including locally generated waves within Willapa Bay.

Evaluation of Model with Field Data

Willapa is a challenging environment in which to apply a wave transformation model. The inlet is subjected to high waves, strong currents, and large variations in water elevation; and the bathymetry at the Willapa entrance is complex and continually changing. Before STWAVE was applied to simulate project alternatives, the model was evaluated with field data to assess the accuracy for such demanding conditions. The initial emphasis of the project was the Middle Channel; thus, wave gauges were deployed at Middle Channel Stations 1, 2, and 3 (see Chapter 4 for discussion of field measurements) to provide verification data. Three verification periods were selected for modeling: 1-4 September 1998, 15-20 October 1998, and 11-16 November 1998. These periods include wave heights of 1.0 to 5.5 m, periods of 4 to 18 sec, offshore wave directions of 205 to 306 deg, peak tidal amplitudes of 1 to 1.5 m, and peak near-bottom currents of 0.5 to 1.2 m/sec. These wave conditions are representative of waves in which vessels navigate through the entrance, as well as the most commonly occurring waves. Measurement accuracy is estimated as

about ±10 percent for wave height and ±10 deg for direction. An evaluation of the pressure gauge record used for the wave measurements is given in Appendix F. The root-mean-square (rms) error in wave height for the pressure gauge, compared with that of a wave buoy, is approximately 0.1 m. The pressure gauge generally underestimates small wave heights (at low tide) and is unbiased at other tide elevations.

Wave transformation at Willapa is sensitive to the minimum water depth across the Willapa bar. The initial attempt to verify STWAVE for the existing Willapa bathymetry produced poor agreement with the measurements. STWAVE gave little wave attenuation between Station 1 and Stations 2 and 3. The lack of agreement called into question the bathymetry data across the Willapa bar. The bar was not surveyed because of the presence of breaking waves, so surveyed depths on either side of the bar were averaged across the bar to give minimum depths of 6 m mtl. Persons knowledgeable about the entrance provided estimates of 1- to 2-m mtl depths in the breaking regions. After modifying the depths across the bar, reasonable agreement was found between STWAVE calculations and the field measurements. STWAVE was initialized with data from the Grays Harbor wave gauge, and the tide was represented with water elevations measured at Station 1.

Comparisons of the calculated and measured wave heights and directions are plotted in Figures 5-5 through 5-10. Statistics are presented in Table 5-6. The calculations tend to overestimate the wave height at low tide at Station 2, although the variation in wave height with the tide is reproduced. The wave directions are modeled well for Station 1, but the calculated directions at Stations 2 and 3 are less variable than measured. The wave directions at Station 2 are more out of the northwest at low tide, when energy from the west is dissipated over the bar and energy reaches Station 2 through the North Channel entrance. At Station 3, wave directions are more from the west at low tide because the energy reaching Station 3 is conveyed through the Middle Channel. The larger errors in wave direction at Station 2 for 12-14 November coincide with strong winds from the south and southeast (as great as 17 m/sec), which generate short-period waves from the south bay. These locally generated waves are not represented in the model. The large uncertainty in the bathymetry over the shoals that front Stations 2 and 3 (because of lack of direct measurements in the breaking regions and sand movement during the interval between the bathymetry surveys and wave measurements) contributes to the model error. Overall, the verification is considered to show reasonable agreement between the calculations and measurements for this energetic and complex environment.

Simulation of Design Alternatives

To evaluate Willapa channel alternatives, two types of wave model simulations were performed. Fifteen representative wave spectra were transformed for ebb, slack, and flood currents to evaluate navigation conditions in the channels. Then, a time-history of waves for a winter month was transformed to provide input for sediment transport estimates.

Table 5-6
Verification Statistics

Date	Sta	Wave Height				Wave Direction	
		Mean Error percent	Mean Error m	rms Error percent	rms Error m	Mean Error deg	rms Error deg
9/1/98-9/4/98	1	6.6	0.10	11.0	0.22	-0.2	2.2
	2	35.1	0.20	45.1	0.23	8.1	14.7
	3	17.1	0.06	31.8	0.09	3.4	12.5
10/15/98-10/20/98	1	-2.4	-0.05	11.5	0.22	-6.7	7.7
	2	25.8	0.13	43.0	0.21	3.8	15.2
	3	17.4	0.07	32.2	0.12	13.3	19.8
11/11/98-11/16/98	1	-3.9	-0.13	11.0	0.37	-7.7	11.3
	2	22.5	0.18	35.3	0.27	15.4	74.3
	3	-22.1	-0.08	26.7	0.10	6.4	8.5

Waves to evaluate navigation

To evaluate the channel alternatives from the perspective of navigability, 15 representative waves were selected. These waves are the most commonly occurring in the wave climate with heights less than 3 m (occurrence greater than 1.5 percent), and account for 70 percent of all wave conditions (85 percent of all waves under 3 m). Only waves less than 3-m cutoff were considered because it is about the limiting wave height to navigate the entrance (see Chapter 2). The 15 waves include incident directions of 225 to 315 deg and periods of 8 to 16 sec. The waves are listed in Table 5-7 with their probability of occurrence.

The navigation evaluation considered five alternatives: Alternative 1 (existing condition), Alternative 3A (existing condition with dredging on the bar), Alternative 3B (North S-Channel), Alternative 4A (Middle Channel), and Alternative 3H (North Channel displaced to the south). Because the navigation evaluation focuses only on the bar channel, these five alternatives cover the range of all North and Middle Channel alternatives. Alterations of the interior channels (except Alternative 4D) resulted in only minor changes to currents in the bar channel (Chapter 6); thus, results for Alternative 4A are representative of 4B, 4C, and 4E. Simulation of the five alternatives included the following steps:

a. The bathymetry grid was modified for each channel alternative as discussed in Chapter 6.

b. Fifteen representative spectra were generated with heights, periods, and directions selected from the wave climate and spectral parameters given in Table 5-4.

c. Typical peak ebb and flood current fields were saved from ADCIRC simulations of each alternative.

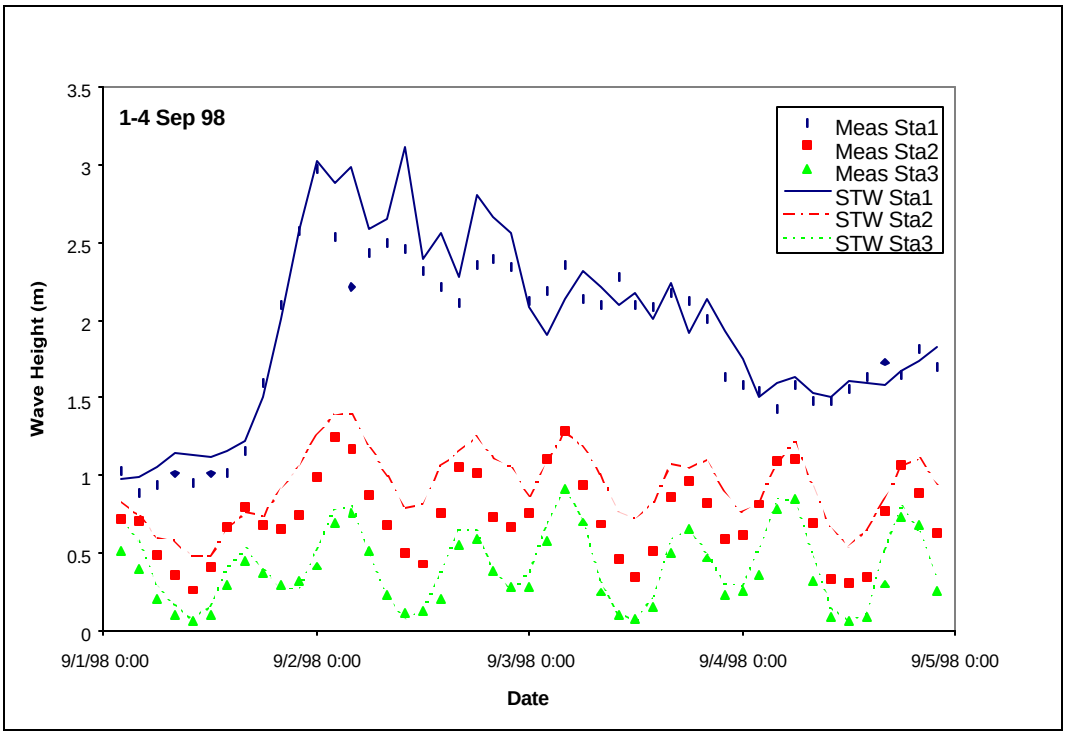

Figure 5-5. Wave height verification for 1-4 September 1998

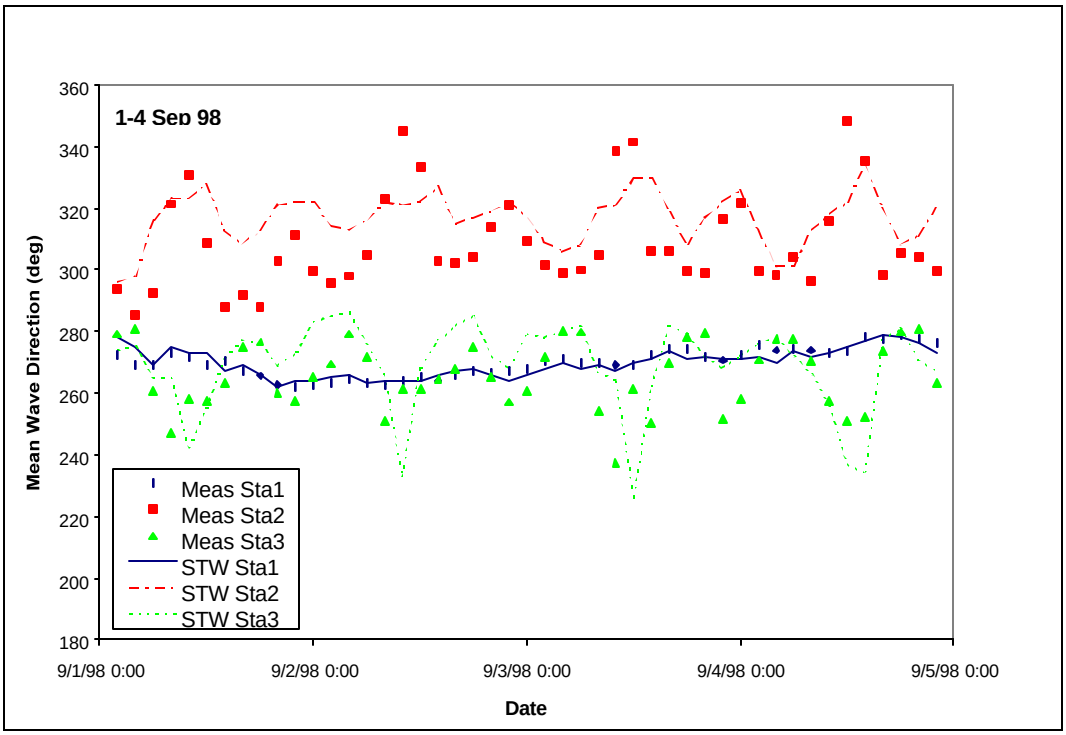

Figure 5-6. Wave direction verification for 1-4 September 1998

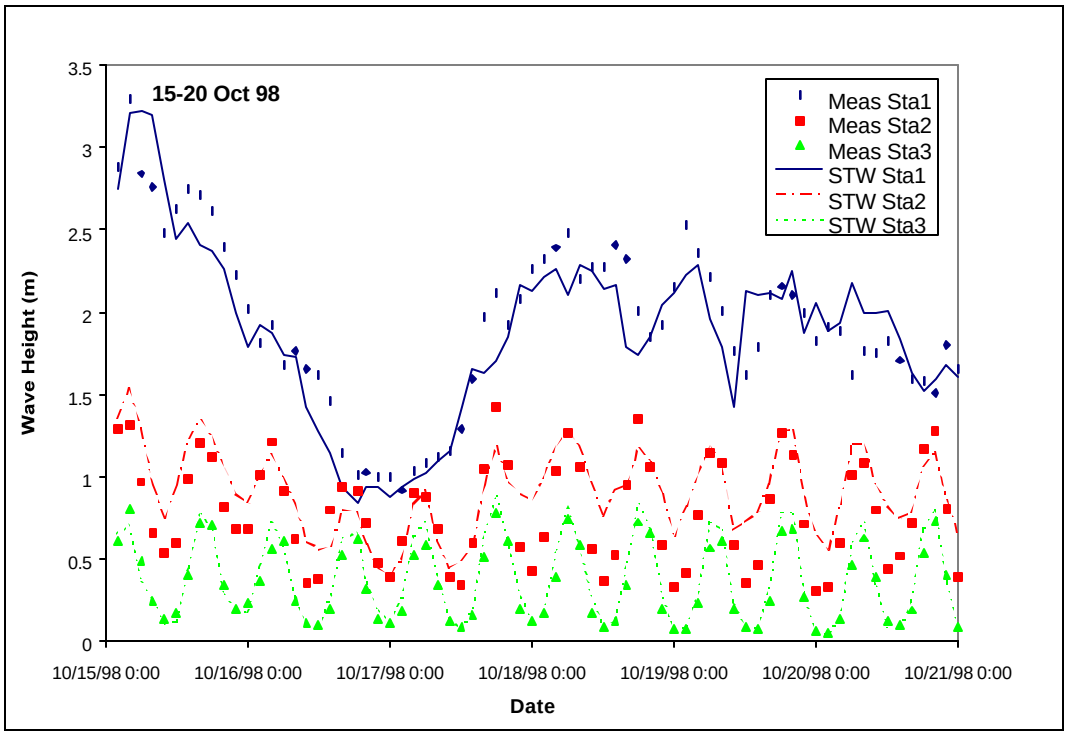

Figure 5-7. Wave height verification for 15-20 October 1998

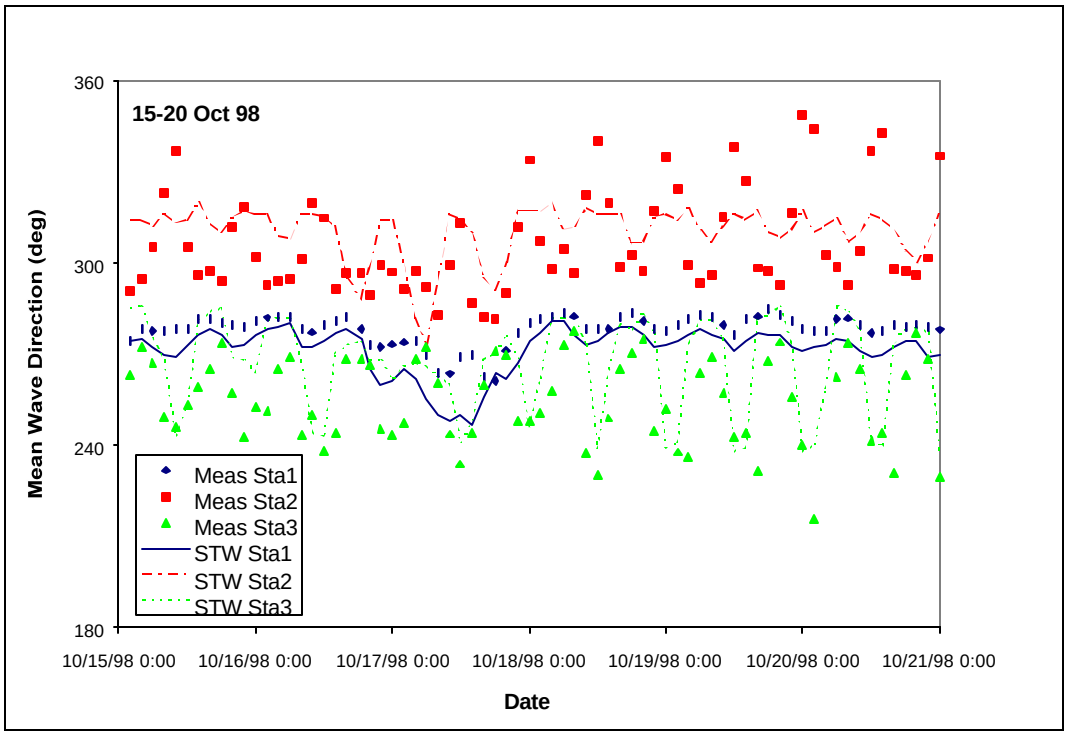

Figure 5-8. Wave direction verification for 15-20 October 1998

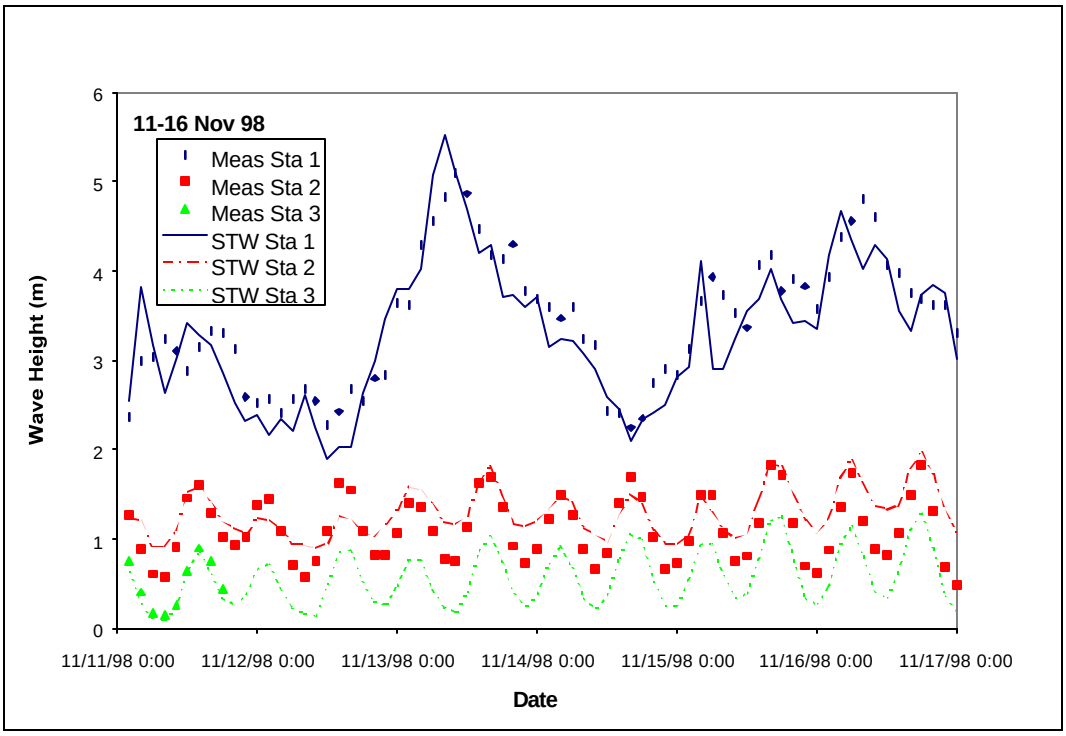

Figure 5-9. Wave height verification for 11-16 November 1998

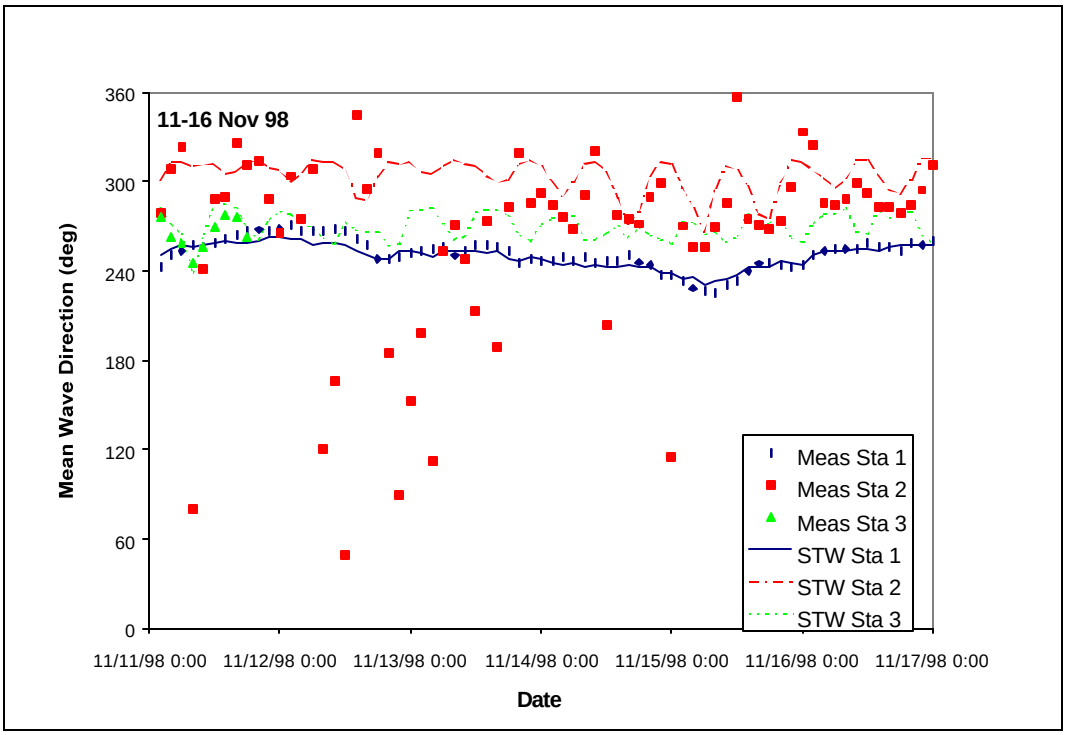

Figure 5-10. Wave direction verification for 11-16 November 1998

d. STWAVE was run to transform the 15 representative waves across each of the bathymetry grids for the five alternatives. Runs were made at mtl with no current, mlw (-1 m) with a typical peak ebb current, and mhw (1 m) with a typical peak flood current. The total number of model runs was 225 (15 waves times three tide/current combinations times five alternatives).

The purpose of the STWAVE navigation-evaluation runs is to compare wave heights and directions in the channels for the five alternatives to identify a preferred alternative. To compare the results, three regions were selected in the entrance channel as the outer channel, midchannel, and inner channel. The outer channel location is the seaward end of each channel, where the channel "daylights" (channel depth equals the longshore depth contour). The midchannel location is the most restricted channel cross section (narrowest width through the shallowest bar section). The inner channel location is bayward of the bar. The locations are separated by distances of 1-2 km. Examples of the wave heights and wave directions (relative to the channel orientation) for the most frequently occurring wave condition (Wave 4 in Table 5-7) are given in Figures 5-11 and 5-12, respectively. Wave heights and directions for ebb, slack, and flood are averaged (heights are generally higher for ebb and lower for flood). In the outer channel and midchannel, the wave heights are similar for the five alternatives. In the inner channel, Alternatives 3B and 3H have significantly higher wave height. The wave directions relative to the local channel orientation are within about ±20 deg in the outer channel and midchannel, but increase to over 60 deg for Alternative 3B and 30 deg for Alternative 4A in the inner channel. The 60-deg obliqueness relative to the channel orientation exceeds the 45-deg window for safe navigation discussed in Chapter 2.

Table 5-7
Representative Waves for Navigation Evaluation Simulations

Wave	H_{mo} m	T_p sec	θ_m deg	Probability Percent
1	1.5	8	225.0	1.5
2	1.5	8	247.5	3.1
3	1.5	8	270.0	10.0
4	1.5	8	292.5	21.6
5	1.5	8	315.0	2.7
6	1.5	12	270.0	5.0
7	1.5	12	292.5	3.3
8	1.5	16	270.0	2.6
9	2.5	8	225.0	1.6
10	2.5	8	270.0	2.6
11	2.5	8	292.5	3.0
12	2.5	12	247.5	1.9
13	2.5	12	270.0	4.8
14	2.5	12	292.5	3.2
15	2.5	16	270.0	2.9

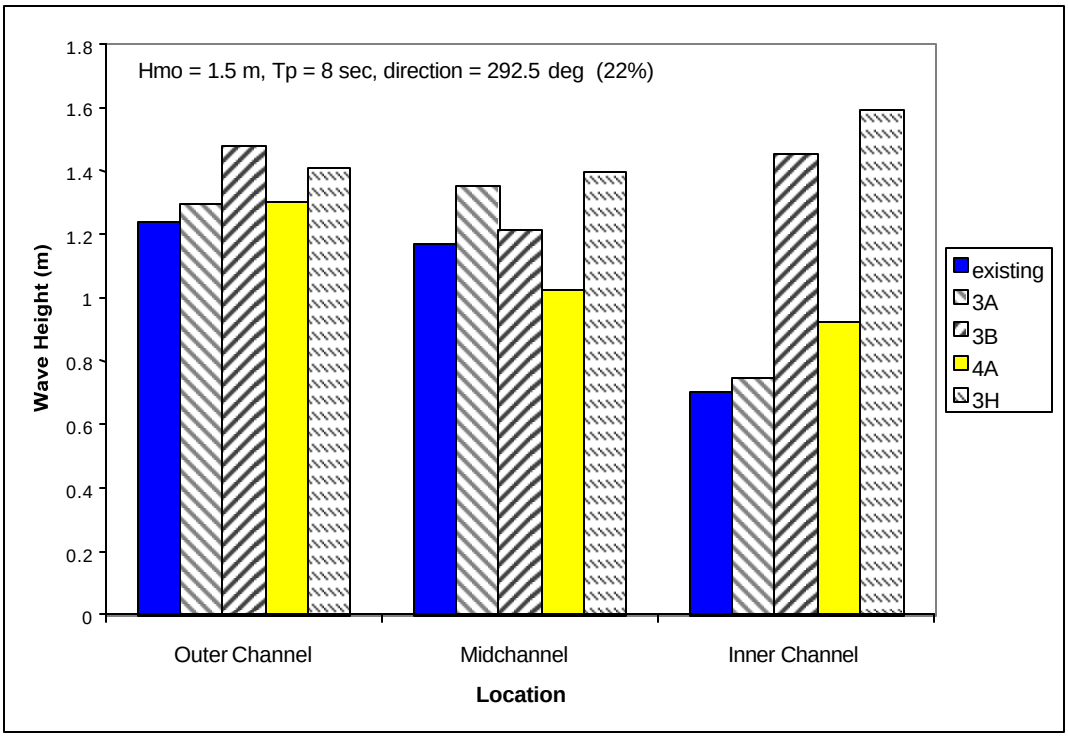

Figure 5-11. Wave height comparison for most frequent wave

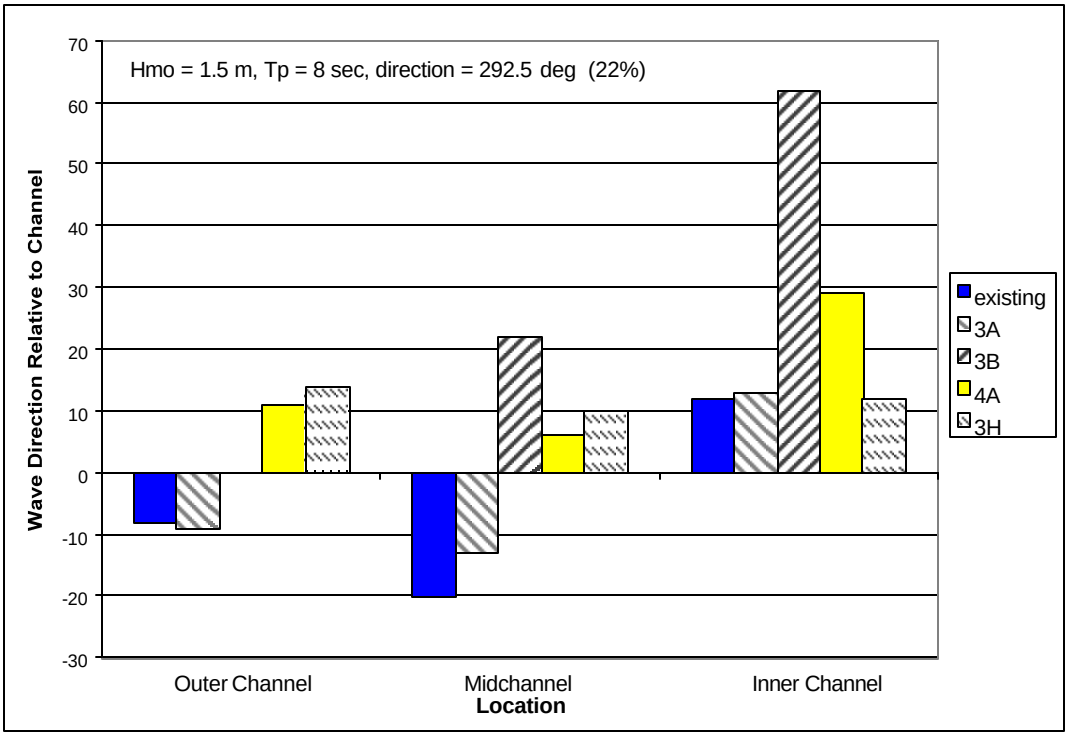

Figure 5-12. Wave direction comparison for most frequent wave

The obliqueness of waves in the inner channel for Alternative 3B is especially problematic because of the higher waves, thus greater wave steepness and potential for wave breaking. Results of averages from the 15 representative waves (weighted by their percent occurrence) are given in Table 5-8. Navigability for any alternative is dictated by the worst conditions that are encountered along the channel. Although Alternative 1 (existing conditions) provides the smallest wave heights, the channel depth is less than the 26-ft design depth (Chapter 2). Alternatives 3A and 4A are similar from the standpoint of waves for navigability. Alternative 3H has significantly higher wave heights in the inner channel than Alternatives 3A and 4A (wave height is approximately double), but has similar characteristics in the outerchannel and midchannel positions. Alternative 3B has poor wave height and direction characteristics in the inner channel.

Alternatives 1 and 3A. The statistics in Table 5-8 show that wave height and direction are fairly consistent between Alternatives 1 and 3A. This is reasonable because these alternatives have the same channel alignment, with a slightly deeper and wider channel in Alternative 3A. The wave height increases 10 to 15 percent for Alternative 3A relative to Alternative 1, because the deepening and widening of the entrance channel increase wave penetration. Wave angles relative to the channel exceed 45 deg in the outer channel or midchannel for about 10 percent of wave conditions less than 3 m (based on the 15 representative waves). Typically, incident wave directions of 247.5 deg and less result in angles greater than 45 deg relative to the outer channel and midchannel.

Alternative 3B. Alternative 3B (S-channel) has the poor characteristics in the inner channel of high wave heights (122 percent of Alternative 1) and wave angles oblique to the channel (51 deg, on average). Wave energy is focused on the inner channel by the entrance bar. Also in the inner channel, the channel orientation is toward the northeast/southwest (230 deg), so dominant incident waves from the west and west-northwest are oblique to the channel. A channel configuration similar to Alternative 3B was the marked channel until recently (October 1998). The difficulties in navigating this channel are the primary motivation of this study. Wave angles relative to the channel exceed 45 deg for about 60 percent of wave conditions less than 3 m. Typically, incident wave directions of 225 deg and less for the outer channel or 292.5 deg and greater for the inner channel result in angles greater than 45 deg relative to the channel.

Table 5-8
Comparison of Wave Height and Direction for Channel Alternatives

Alternative	Average H_{mo} M			Increase in H_{mo} Relative to Alternative 1 percent			Average $_m$ Relative to Channel Orientation deg		
	Outer	Mid	Inner	Outer	Mid	Inner	Outer	Mid	Inner
1 existing	1.5	1.5	0.8	0	0	0	19	30	9
3A	1.6	1.7	0.9	9	15	9	20	23	10
3B	1.8	1.5	1.9	24	4	122	15	15	51
4A	1.7	1.4	1.1	17	-8	44	12	8	26
3H	1.7	1.8	1.9	14	10	158	14	10	11

Alternative 4A. Alternative 4A (Middle Channel) generally has higher wave heights in the outer and inner channels and lower heights in the midchannel compared with Alternatives 1 and 3A. The wave angles are generally less oblique in the midchannel, but more oblique in the inner channel. The reason for increased wave height and more oblique wave directions in the inner channel for Alternative 4A is that wave energy enters the region of the North Channel and is refracted and diffracted into the inner reach of the Middle Channel. For Alternatives 1 and 3A, wave energy is sheltered in the inner channel by Cape Shoalwater. Wave directions do not exceed 45 deg for the representative wave conditions.

Alternative 3H. Alternative 3H generally has similar wave heights and directions in the outer channel and midchannel to those of Alternatives 1 and 3A. But, the wave height is approximately double that of Alternatives 1 and 3A in the inner channel. The wave angles are generally slightly less oblique in the outer channel and midchannel. The reason for increased wave height in the inner channel for Alternative 3H is that wave energy is focused by the ebb shoal and interior shoals and there is less sheltering from Cape Shoalwater to the north (compared with Alternatives 1 and 3A). Wave directions do not exceed 45 deg for the representative wave conditions.

Navigability is a function not only of wave height and direction, but also of wave steepness (ratio of wave height to wavelength) and wave breaking. Steeper waves increase potential for a vessel to be overturned or swamped. Waves steepen in shallow water because wavelength decreases and height increases through refraction and shoaling. Similarly, waves steepen on ebb currents. For each of the alternatives, ebb and flood current magnitudes and channel depths are similar, so wave steepnesses are also similar (except the inner channel of 3B and 3H, where wave height and thus steepness can double). Wave breaking is also a function of wave height, wave steepness, and water depth. Thus, the wave-breaking characteristics of Alternatives 1, 3A, and 4A are expected to be similar. Alternatives 3B and 3H would experience increased breaking in the inner channel, where wave heights are higher than with the other alternatives. STWAVE can estimate regions of increased steepness or wave breaking, but not the timing or location of individual steep or breaking waves that might cause difficulty for navigation.

This study focused on waves in the bar channel, but results show that there are differences in wave height between the bay portions of the North and Middle Channels, also. At high tide (flood), waves are smaller in the bay portion of the North Channel than in the Middle Channel because of sheltering from Cape Shoalwater. At low tide (ebb), waves are slightly smaller in the bay portion of the Middle Channel because most of the wave energy is dissipated on the bar. Because vessels generally navigate through the outer bar on flood, near high tide, the North Channel alternatives offer decreased wave action in the interior bay channel, compared with that of the Middle Channel.

Detailed plots of the wave height and direction for the outer channel, midchannel, and inner channel for each alternative are given in Appendix D. Ebb, slack, and flood simulations for each wave are displayed separately.

Waves to evaluate sediment transport

To support sediment transport modeling, nearshore wave fields for one typical winter month were required. The month of January 1998 was selected because the Grays Harbor buoy record was continuous, and the mean wave height was near the mean winter wave height at the buoy (3.2 m for January 1998 versus 3.0 m for all winter months). A time-history of Grays Harbor measurements for January 1998 is given in Figure 5-13 (other winter months are plotted in Appendix C). STWAVE simulations were made with input every 3 hr from the Grays Harbor buoy, for a total of 248 model runs. Tide elevations were taken from the NOS Toke Point gauge. Tidal currents were neglected in the wave simulations because sensitivity tests showed that wave height and direction variation produced by the wave-current interaction were localized and would have minor influence on sediment transport calculations. The wave- and current-driven sediment transport calculations are discussed in Chapter 6.

Summary

The wave transformation model STWAVE was applied to calculate wave heights and directions at the entrance to Willapa Bay. The model resolution was 100 m and covered a domain of 30 by 51 km. The model was driven with input wave information from the Grays Harbor wave buoy. Field measurements taken at three stations in the mouth of Willapa Bay were used to evaluate the model for application to the complex environment of Willapa entrance. Verification results showed reasonable agreement between calculations and measurements at three locations where measurements were available. The model was applied to compare relative differences in wave height and direction for different channel alternatives.

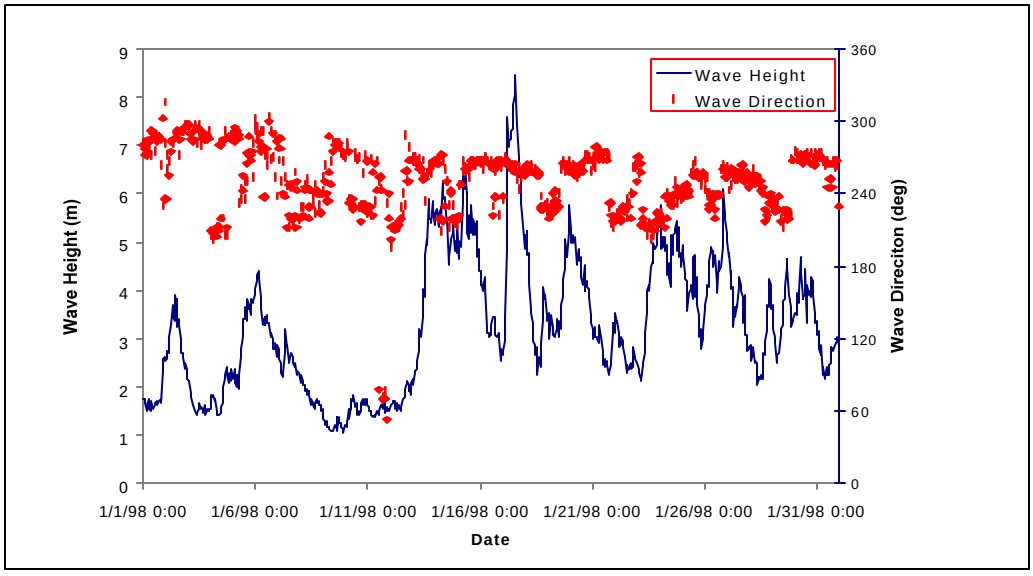

Figure 5-13. Grays Harbor measurements for January 1998

Following verification, five channel alternatives for Willapa Bay, Alternatives 1, 3A, 3B, 4A, and 3H, were evaluated. For each alternative, the model was run for 15 representative waves at ebb (mlw), slack (mtl), and flood (mhw). From the perspective of navigation, the following conclusions are made based on the short-wave modeling:

a. Alternatives 1 and 3A give equivalent results within the accuracy of the model. Wave heights for Alternative 3A are slightly higher (9-15 percent) because more wave energy can penetrate the deeper and wider entrance channel. Wave directions (relative to the channel axis) in the outer channel and midchannel exceed 45 deg for waves incident from the southwest and west-southwest. These North Channel alternatives have lower wave heights in the bay channel during high-tide conditions because wave energy is sheltered by Cape Shoalwater.

b. Alternative 3B gives consistently higher wave heights and more oblique wave directions (relative to the channel orientation) than Alternatives 1 and 3A. The higher waves also imply larger wave steepnesses and more frequent wave breaking. In the inner channel, wave directions would often exceed 45 deg, and typical wave heights would be near 2 m (compared with less than 1 m for Alternatives 1 and 3A), making Alternative 3B less preferable for navigation.

c. Alternative 4A gives results similar to those of Alternatives 1 and 3A, but the wave height is slightly higher in the outer and inner parts of the channel (17 and 44 percent, respectively, compared with Alternative 1), but lower in the midchannel (8 percent compared with Alternative 1). Wave angles tend to be less oblique than Alternative 1 in the midchannel, but more oblique in the inner channel. Waves at the inner channel for Alternative 4A are higher and more oblique because the Middle Channel is not naturally sheltered by Cape Shoalwater, and wave energy entering through the North Channel is refracted and diffracted around the Willapa bar to the inner channel region. Wave directions for the 15 representative waves do not exceed 45 deg in the Middle Channel.

d. Alternative 3H gives consistently higher wave heights in the inner channel compared with Alternatives 1 and 3A. The higher waves also imply larger wave steepnesses and more frequent wave breaking. The wave directions for Alternative 3H are generally less oblique to the outer channel and midchannel, than with Alternative 1 and 3A. Although the wave characteristics of Alternative 3H do not violate the navigation criteria, the larger interior wave heights would result in more difficult navigation over a longer distance in the entrance channel.

The STWAVE simulations do not show a clear preference for Alternative 1, 3A, or 4A based on navigation criteria of wave height and wave direction relative to the channel, within the accuracy of the model. Alternatives 3B and 3H are relatively less preferable because of the high waves (and oblique wave directions for Alternative 3B) in the inner channel.

Wave fields were also calculated for a typical winter month. STWAVE was run every 3 hr with input from the Grays Harbor buoy for January 1998. These STWAVE results are applied in Chapter 6 for sediment transport calculations.

References

Bouws, E., Gunther, H., Rosenthal, W., and Vincent, C. L. (1985). "Similarity of the wind wave spectrum in finite depth waves; 1. Spectral form," *Journal of Geophsyical Research* 90(C1), 975-986.

Corson, W. D., Abel, C. E., Brooks, R. M., Farrar, P. D., Groves, B. J., Payne, J. B., McAneny, D. S., and Tracy, B. A. (1987). "Pacific coast phase II wave information." WIS Report 16, U.S. Army Engineer Waterways Experiment Station, Vicksburg, MS.

Lillycrop, W. J., Parson, L. E., and Irish, J. L. (1996). "Development and operation of the SHOALS Airborne Lidar Hydrographic Survey System," SPIE: *Laser remote sensing of natural waters - from theory to practice* 2964, Proceedings, International Society for Optical Engineering. V. I. Feigels and Y. I. Kopilevich, eds., 26-37.

Resio, D. T. (1987). "Shallow-water waves. I: Theory," *Journal of Waterway, Port, Coastal, and Ocean Engineering* 113(3), ASCE, 264-281.

_____. (1988). "Shallow-water waves. II: Data comparisons," *Journal of Waterway, Port, Coastal, and Ocean Engineering* 114(1), ASCE, 50-65.

Smith, J. M., Resio, D. T., and Zundel, A. K. (1999). "STWAVE: Steady-state spectral wave model; Report 1: User's manual for STWAVE version 2.0," Instructional Report CHL-99-1, U.S. Army Engineer Waterways Experiment Station, Vicksburg, MS.

Thompson, E. F., Hadley, L. L., Brandon, W. A., McGehee, D. D., and Hubertz, J. M. (1996). "Wave response of Kahului Harbor, Maui, Hawaii," Technical Report CERC-96-11, U.S. Army Engineer Waterways Experiment Station, Vicksburg, MS.